Simulation & validation of delamination growth in CFRP specimens under mixed mode loading using cohesive elements

S Nadeem Masood[a], Arun Kumar Singh and S R Viswamurthy
[a]*corresponding author Tel: 080-25086936, E-mail address: nadeemmasood@nal.res.in*
Advanced Composites Division, National Aerospace Laboratories, Council of Scientific and Industrial Research, Bangalore, India

Abstract

This paper discusses in detail the use of cohesive interface elements for simulation of delamination growth in composites. The work addresses the complexities in the convergence of numerical simulations that arise due to cohesive elements. A systematic way to obtain the best values for cohesive element parameters while finding a balance between accuracy of the results, computation time and numerical stability is presented. Parametric studies on cohesive elements are conducted through simulation of the standard Double cantilever beam (DCB) test in Abaqus/standard and numerical results are validated with test data. The optimized parameters are used to simulate the end-notched flexure (ENF) test and mixed-mode bending (MMB) tests. Numerical results for the above tests are in good agreement with the test data, thereby validating our approach.

Keywords: Abaqus; Cohesive interface elements; delamination; double cantilever beam

1. Introduction

The application of laminated carbon fibre reinforced polymer (CFRP) composites is expanding due to its excellent specific strength and stiffness. Delaminations and disbonds are major concerns in laminated composites due to their poor interlaminar properties. The tendency of composites to delaminate/disbond has caused concern amongst the designers to have effective numerical simulation model which can predict their onset and/or its growth. Also, prediction of delamination / disbond growth in composite structures under complex loading conditions through numerical simulations is important for damage tolerance evaluation. A detailed status report on delamination resistance testing under the frame work of fracture mechanics can be found in Ref. [1]. Numerical methods for crack propagation such as virtual crack closure techniques (VCCT) [2, 3], modified VCCT [3, 4], Virtual crack extension [5] and J-integral [4, 5] can be used to predict delamination growth. These methods are based on the assumption that the available strain energy release rate at the delamination front is greater than or equal to a critical value strain energy. However, these methods face some convergence issues and require high computation time when applied in finite element codes. A relatively new and effective method for prediction of delamination/disbond onset and growth within the framework of damage mechanics is cohesive zone model (CZM). CZM can be used to predict both the initiation of a new crack and growth of an existing crack. CZM is widely used in finite element tools for interfacial failure or disbond/delamination modeling [6, 7, 8].

This paper discusses in detail the use of cohesive interface elements [9] for numerical simulation of disbond growth in standard interlaminar fracture toughness tests for mode-I, mode-II and mixed mode-I/II tests. The numerical modeling and simulations are conducted using the finite element tool Abaqus/Standard [9]. CFRP test coupons were fabricated using IMA/M21 prepreg using autoclave moulding process. Interlaminar fracture toughness tests were conducted under pure mode-I, pure mode-II and mixed mode-I mode-II loading. Test data was used for development of numerical simulations and their validation. Mode-I, mode-II and mix mode-I mode-II fracture toughness tests are conducted as per ASTM D5528, ASTM D7805 and ASTM D6671 [10, 11, 12]. The test procedure and fracture toughness calculations are not presented in current work since it is well defined in open literature. However, a brief detail of all tests and measured fracture toughness is presented and this detail can be found in [13]. Figure 1 presents the fracture toughness contour for IMA/M21 Carbon fiber composite. This figure includes data from all fracture toughness tests; Pure mode-I DCB tests (G_{II}/G_T=0), pure mode-II ENF tests (G_{II}/G_T =1) and mixed mode-I/II tests at seven different ratios (G_{II}/G_T = 25%, 30%, 40%, 50%, 55%, 60% and 69%). At least 3 specimens were tested in each MMB specimen case. Figure 1 also presents a conservative curve fit obtained using Benzeggagh-Kenane (B-K) law [14]and the measured fracture toughnesses G_{IC} = 325 J/m^2, G_{IIC} = 2492 J/m^2. The parameter η is 2.193 calculated by applying least error-square fit to the curve. Failure is expected when, for a given mixed-mode ratio G_{II} /G_T, the calculated, G_T exceeds the G_C. This data is used for development and validation of numerical simulation for DCB, ENF and MMB test.

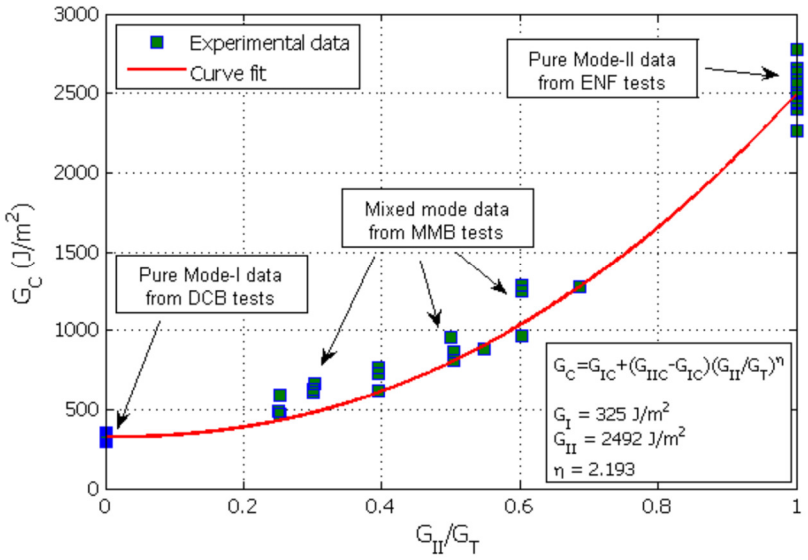

Figure 1: Interlaminar fracture toughness contour for IMA/M21 prepreg material [13]

Nomenclature

G_C	critical strain energy release rate / fracture toughness
G_T	total strain energy release rate
G_{IC}	fracture toughness in pure mode-I direction
G_{IIC}, G_{IIIC}	fracture toughness in pure mode-II and mode-III direction
η	exponent in B-K law
K_{NN}, K_{SS} and K_{TT}	elastic parameters for traction-separation law in the normal direction and the two shear directions
N_{max}, S_{max}, T_{max}	maximum stresses for traction-separation law in the normal direction and the two shear directions
ΔLc	characteristic length of the cohesive element
t_{ply}	cured ply thickness

1.1. Cohesive zone model theory

The concept of cohesive element was introduced from analysis of crack growth in concrete by Hillerborg [15]. Further, cohesive element modeling was extended to a wide variety of material from metal, polymer, ceramics to fibre reinforced polymer [16, 17]. With the increased application of cohesive element, a finite element tool Abaqus version 6.5 [18] onwards has commence 'cohesive element modeling' in both standard (implicit) and explicit solution procedures. This enables the user to model a defined plane of finite or zero thickness where the crack is expected to develop in the structure. The interface response in cohesive element modeling is defined by parameters such as fracture energy which can be obtained from fracture toughness test. The constitutive response of these elements depends on the specific application and is based on certain assumptions about the deformation and stress states that are appropriate for each application area. Traction-separation-based modelling is usually opted for these simulations as it is best suited [9]. Response of the traction-separation law is defined within the same general framework used for conventional materials (Figure 2). The traction-gap opening behaviour of a cohesive element follows a linear path governed by its elastic parameters K_{NN}, K_{SS} and K_{TT}. Once the traction reaches the nominal value of N_{max}/ S_{max}/ T_{max} the stiffness of the element reduces gradually. The element follows a linear (or exponential) degradation post-initiation response. At the point when the stiffness of the element becomes zero, the work done to completely degrade this element is the fracture energy G_C (Figure 2). The element now acts only as a contact region to deny any physically impermissible cross-over of the two substructures to which the cohesive zone is bonded. The element fails completely at a displacement δ_{fail}. The relationships between these parameters are better explained in the Figure 2.

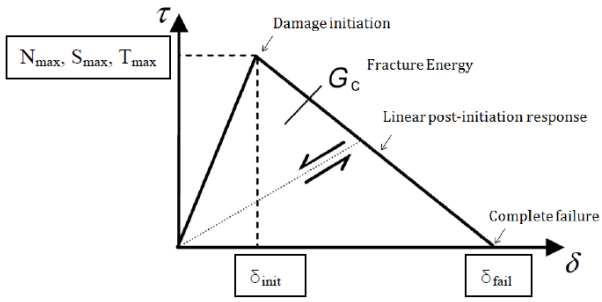

Figure 2: Traction-separation law for cohesive elements

All the above cohesive element parameters are material dependent and can be calculated from equations given below.

$$N\,max = 2\,\frac{GIC}{\delta fail} \qquad \text{Equation 1}$$

$$S\,max = T\,max = 2\,\frac{GIIC}{\delta fail} \qquad \text{Equation 2}$$

$$K\,nn = 2\,\frac{GIC}{\delta ratio \times \delta fail^2} \qquad \text{Equation 3}$$

$$K\,ss = Ktt = 2\,\frac{GIIC}{\delta ratio \times \delta fail^2} \qquad \text{Equation 4}$$

Where, penalty factor= $\delta_{fail}/\Delta L_c$ and $\delta_{ratio}= \delta_{init}/\delta_{fail}$. G_{IC} and G_{IIC} are the fracture energies measured from mode-I and mode-II fracture toughness tests. G_{IIIC} is assumed to be equal to G_{IIC}. ΔLc is decided by the over meshing factor (OMF). OMF is the ratio of structural mesh to cohesive zone mesh. The cohesive zone mesh can be finer than the surrounding structural mesh. It should be at most 5 times smaller than the structural mesh and anything more does not increase accuracy of the solution [19]. If the structural mesh is fine enough, no over meshing of the cohesive zone mesh is required. The Penalty factor can be 0.05 as an initial guess. This can be increased if numerical convergence issues are encountered. This factor should be kept as low as possible for achieving good convergence during simulations. The value of δ_{ratio} suggested by Diehl et al [20] is 0.5, as this ratio is lowered, the elastic values increase slightly, but in general δ_{ratio} does not play a very significant role in the simulations.

1.2. Damage initiation and evolution law for cohesive elements

Cohesive elements are generally governed by a damage law which controls damage initiation and evolution. In the analyses presented herein, the energy-based Benzeggagh and Kenane (B-K) damage evolution criterion shown in Equation 5 is used [14]. In a general load case scenario, there could be a combination of mode-I/II thus mixed mode B-K criteria is used for damage evolution. Interface failure is expected when, for a given mixed-mode ratio G_{II}/G_T, the G_T exceeds the G_C.

$$G_{IC} + (G_{IIC} - G_{IC})\left(\frac{G_{II}}{G_T}\right)^{\eta} = G_T \qquad \text{Equation 5}$$

It is assumed that the onset of damage can be predicted by quadratic normal stress criterion. Damage is assumed to initiate when nominal stress ratios reaches a value of 1 given in Equation 6 [9].

$$\left(\frac{N}{N_{max}}\right)^2 + \left(\frac{S}{S_{max}}\right)^2 + \left(\frac{T}{T_{max}}\right)^2 = 1 \qquad \text{Equation 6}$$

2. Parametric study of Cohesive elements from simulation of DCB test

It is important to use proper stiffness definition of cohesive elements in numerical simulation of delamination or disbond. Cohesive element poses numerical convergence issues if softening constitutive model stiffness is not optimized. Furthermore, cohesive parameters like penalty factor and δ_{ratio} affect computation time, accuracy of results and output file size. In order to determine the optimal values of cohesive element parameters, the double cantilever beam (DCB) specimen test was simulated using cohesive elements for propagation of disbond and validated with test data. The stress and stiffness for cohesive elements in opening mode were calculated from

the fracture toughness measured from test data using Equation 1 to 4.

The material properties and dimensions of DCB specimen used in modelling are given in Table 1 and Figure 3 respectively. The laminate consists of 20 plies (all 0° orientation), with the initial delamination at the mid plane. The finite element model of the DCB specimen was developed using the pre-processor Abaqus/CAE. The specimen is composed of two sub-laminates, each 1.80 mm thick. The initial crack length (a_o) is 55 mm.

Table 1: Material Properties of IMA/M21 Prepreg

E_{11}	149 Gpa
E_{22}	10 Gpa
G_{12}	5.2 Gpa
V_{12}	0.302
t_{ply}	0.182 mm

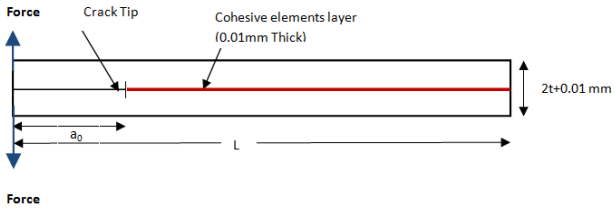

Figure 3: Schematic of DCB specimen FE model

Each sub-laminate was modelled with 4-noded shell elements (S4R). A layer of 8-noded cohesive element (COH3D8) was modelled at mid plane next to the pre-crack region to simulate progressive damage growth under mode-I loading. Top and bottom faces of cohesive element layer were tied to the shell elements using tie constraints. The thickness of cohesive elements was taken as 0.01 mm. Opening displacement was enforced on one half of the specimen through the use of multi point tie constraints and reaction force was measured at other hinged end. Viscosity parameter of $1x10^{-5}$ was used for cohesive elements in order to aid the convergence of simulation in the non-linear region. This value was selected based on authors' experience. An OMF of 5 was considered as suggested by Diehl [19]. A mesh convergence study was conducted first while assuming penalty factor and δ_{ratio} to be 0.05 and 0.5 respectively.

In order to reduce the computation time an optimum mesh size needs to be chosen which gives reasonably accurate results. For mesh refinement study, five different structural mesh sizes were considered. The mode-I interlaminar fracture toughness measured from DCB test (328 J/m^2) and mode-II fracture toughness measured from ENF test (2492 J/m^2) was consistently used to calculate the cohesive elements parameters given in Equation 1 to Equation 4. Five different models were studied and they were named DCB M-1, DCB M-2, DCB M-3, DCB M-4 and DCB M-5. The Quadratic stress criterion (Equation 6) was used to predict damage initiation in the cohesive elements. The reaction force for all above models is plotted against applied displacement and compared with test data (SP1-SP5) in Figure 4.

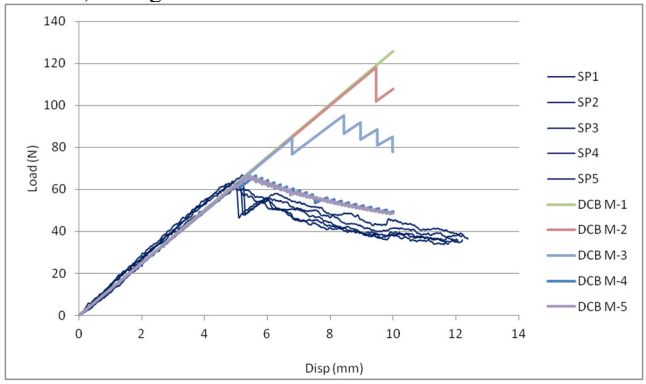

Figure 4: Comparison of DCB experimental data and numerical simulation for different mesh sizes

The number of elements in model and corresponding computational time are presented in Table 2 in decreasing order. The analyst has to compromise on the accuracy vis-à-vis computational time and output data file size. Based on the results shown in Figure 4 and Table 2, the model DCB M-4 appears to be best choice.

Thus, 1mm x1mm structural mesh size and 0.2mm cohesive mesh is used in parametric studies.

Table 2: Output of mesh dependency sensitivity study

Model Name	Shell Element Size (mm)	Cohesive Element size (mm)	Total No. of Elements	CPU time (hrs)	output file size
DCB M-5	0.5x0.5	0.1x0.1	186500	160	140 GB
DCB M-4	1x1	0.2x0.2	46625	16.7	15.6 GB
DCB M-3	2x2	0.4x0.4	11763	2.3	1.61 GB
DCB M-2	3x3	0.6x0.6	5176	0.32	327 MB
DCB M-1	5x5	1x1	1865	0.03	78.6 MB

2.1. Sensitivity to δ_{ratio}

Model DCB M-4 was considered for optimization of δ_{ratio}. A δ_{ratio} of 0.5 was assumed in previous section. Three more δ_{ratio} were chosen to study the effect of δ_{ratio}. Stiffness and strength values of cohesive elements were updated for the new δ_{ratio}. The reaction force for all above models is plotted against applied displacement and compared with test data in Figure 5.

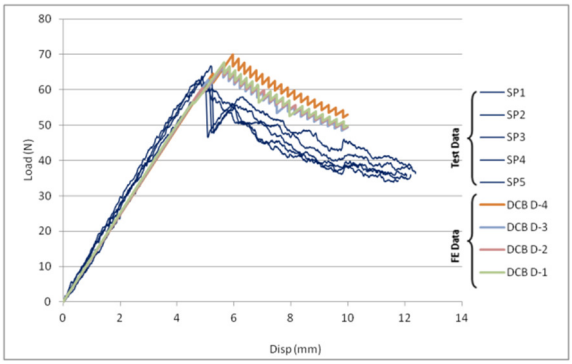

Figure 5: Comparison of DCB experimental data and numerical simulation for different δ_{ratio}

Table 3: Output of δratio sensitivity study

Model Name	Del Ratio	Penalty factor	CPU time (hrs)	Output file size
DCB D-4	0.8	0.05	20	20 GB
DCB D-3	0.5	0.05	16.7	15.6 GB
DCB D-2	0.3	0.05	18.5	16 GB
DCB D-1	0.1	0.05	13.4	11.1GB

From Table 3 and Figure 5 it is observed that the solution converges with δ_{ratio} of 0.5. Further reducing the δ_{ratio} does not improve the results significantly. Hence, δ_{ratio}=0.5 is used in all further simulations.

2.2. Sensitivity to Penalty Factor

Further, model DCB D-3 is used to study the effect of penalty factor. A penalty factor of 0.05 was assumed for this model. Three more penalty factors were chosen to study the effect of penalty factor i.e. 0.065, 0.08 and 0.1. The cohesive element properties (stress and stiffness) were updated for the new penalty factors in all 4 models. The reaction force for all above models is plotted against applied displacement and compared with test data in Figure 6.

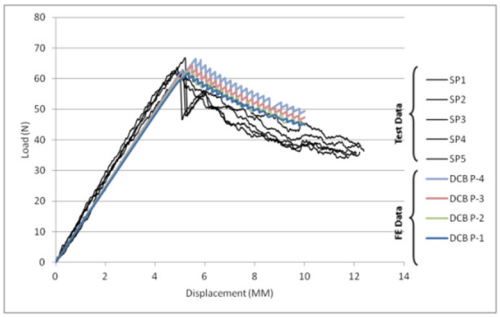

Figure 6 Comparison of DCB experimental data and numerical simulation for different penalty factors

From Figure 6 and Table 4 it is clear that with the increase of penalty factor, the solution converges. Moreover, CPU time and output database file sizes are reduced. Penalty factors of 0.08 and 0.1 give almost same accuracy. Thus model DCB P-2 (penalty factor 0.08) was considered the best among the other penalty factors. As the mesh size is 1mm x 1mm for all the models thus the total numbers of elements comes out to be 46625.

Table 4: Output of penalty factor sensitivity study

Model Name	Penalty factor	CPU time (hrs)	Output File Size
DCB P-4	0.05	16.7	15.6 GB
DCB P-3	0.065	10	16.5 GB
DCB P-2	0.08	7.3	10.4 GB
DCB P-1	0.1	6.8	11.3 GB

Based on the parametric study, the final refined parameters are presented in Table 5. These two optimized parameters will be consistently used for all the further simulations in next section. The reaction force against applied displacement using refined values is presented in DCB P-2 in Figure 6.

Table 5: Optimized cohesive element parameters

Cohesive element parameter	Refined value
Penalty factor	0.08
δ_{ratio}	0.5

3. Modeling & Numerical Simulation of ENF Test

The finite element model of the ENF specimen was also developed using the pre-processor Abaqus/CAE. The specimen is composed of two sub-laminates, each 1.7 mm thick. The initial crack length (a_o) is 41 mm and total laminate length (L) is 120 mm and width (w) is 25mm. Each sub-laminate has a stacking sequence of $[0_{10}]$. The configuration of the specimen is shown in Figure 7 along with the boundary conditions applied.

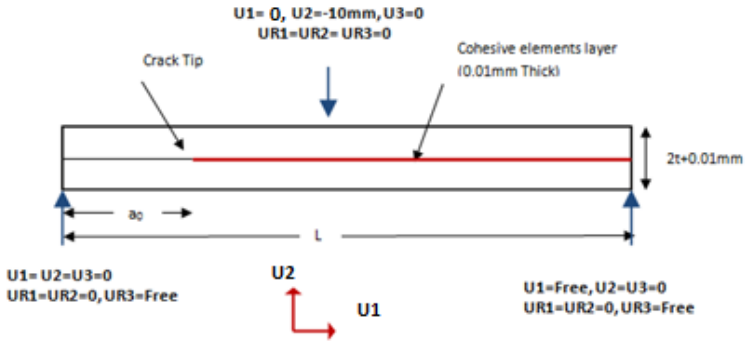

Figure 7 Schematic of ENF specimen model

Optimized cohesive element parameters (Table 5) and Mode-II fracture toughness (from Figure 1) were used for calculating the cohesive element properties for ENF model (using equations 1 to 4 The total number of structural (S4R) elements of 1mmx1mm size and 3D cohesive elements (COH3D8) of 0.2mmx0.2mm size used were 6000 and 49375 respectively. The material properties for ENF simulation were taken same as in Table 1 except for E_{11} which is now taken as 118 GPa. This change in E_{11} was due to observations made during material characterization tests. The standard 3-point bending short beam tests conducted on IMA/M21 prepreg specimens exhibited a much lower stiffness (E_{11}=118 GPa) compared to standard tensile specimen tests (E_{11}=149 GPa).

The same was followed for MMB test simulation described in next section. The plot of reaction load (RF2) versus applied displacement (U2) is generated from simulation output and compared with experimental data (Figure 8). It is clear that numerical simulation matches well with test data. The initial stiffness of the specimen is captured well in simulation. The sudden, unstable onset of delamination growth observed in test is also captured in the simulation to a good extent.

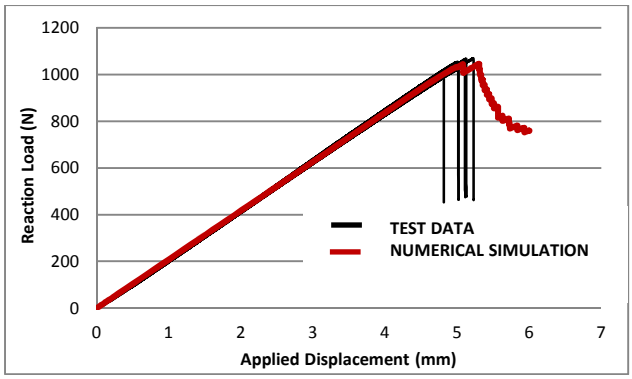

Figure 8: Comparison of reaction load vs. applied displacement for ENF test and numerical simulation

The numerical simulation of ENF test typically takes about 10 hours of CPU time and generates an output file size of about 8GB. Figure 9 shows the contour of SDEG parameter (stiffness degradation in cohesive elements; SDEG=0 means element is undamaged) at an arbitrary interval which shows the state of damage in an element [9]. The region coloured red in the figure shows the disbond/crack growth from initial position; blue coloured region indicates the region where specimen is still bonded. A maximum of 95% degradation in the stiffness of cohesive elements was allowed; beyond which stiffness of the element was kept constant.

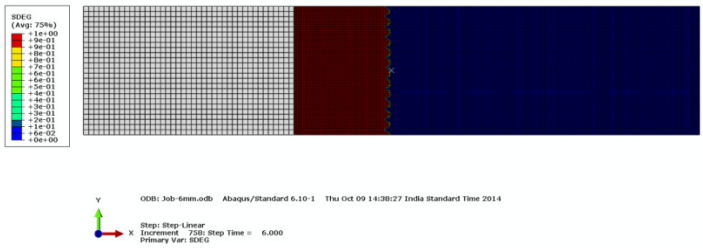

Figure 9: FE Model of ENF specimen shows SDEG contours

4. Modeling and Numerical Simulation of MMB Test

The laminate consists of 20 plies (all 0° orientation), with the initial delamination at the mid plane. The specimen was composed of two sub-laminates each 1.67 mm thick. The initial crack length (a_o) is 27.5 mm and the total specimen length (L) is 100mm and width (w) is 25mm. Each sub-laminate has a stacking sequence of $[0_{10}]$. In MMB test, crack growth is unstable and specimen is assumed to have failed once crack growth initiates. The cohesive element layer was modeled only up to 10mm from crack tip along the length of specimen. Different G_{II}/G_T ratios are simulated by applying different displacement boundary conditions using kinematic coupling feature available in Abaqus/standard. The advantage of kinematic coupling is that different mode ratios can be simulated simply by changing the length 'c' of loading lever [9]. A schematic of the developed numerical model (specimen, interface elements and applied boundary conditions) is shown in Figure 10. The green line the Figure 10 represents loading lever which is connected to the specimen with hinged boundary conditions. Loading lever transferred only load without generating any moment at the connection.

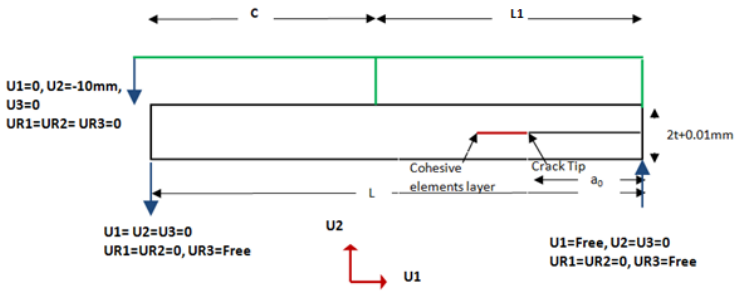

Figure 10: Schematic of MMB FE model

Optimised cohesive element parameters (Table 5) were used for the calculating the cohesive element properties for MMB model form equation 1 to 4. The model of MMB specimen uses 5000 structural (S4R) elements and 6250 cohesive elements (COH3D8). The plot of reaction load (RF2) versus applied displacement (U2) for different mode ratios were generated from numerical simulation for all load cases and compared with experimental data. Figure 11 shows the comparison between the predicted and the experimentally determined load-displacement data. An offset of 2 mm on displacement axis is provided in between all cases for the sake of clarity. A good agreement between the experimental and the numerical prediction is obtained. The experimental result obtained in MMB test shows more pronounced and deep drop in stiffness than numerical prediction. This is due to the fact that, numerical simulation faces convergence issues for simulation of sudden drop in stiffens and requires high computation time. Thus, the FE analysis were forcefully terminated once crack start to grow.

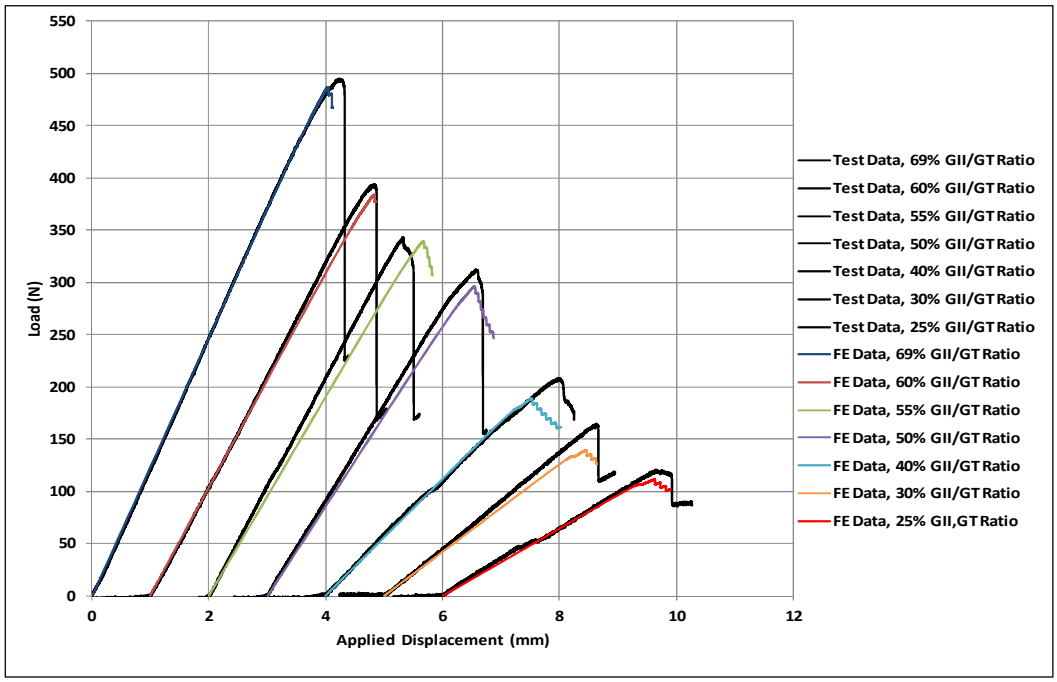

Figure 11: Comparison of reaction load vs. applied displacement for MMB test and numerical simulation

The numerical simulation of MMB test typically takes about 50 hours of CPU time and generates an output file size of about 8GB. Figure 11 shows the SDEG (scalar degradation) of contours and the region coloured red in the figure shows the disbond/crack growth from initial position; blue coloured region indicates the region where specimen is still bonded.

5. Conclusion

A method is presented for the prediction of crack growth in CFRP specimens under pure mode-I, pure mode-II and mix mode-I/II using Abaqus cohesive elements. Fracture toughness tests are conducted for all cases and calculated fracture toughness is used to develop numerical models. Cohesive element parameters δ_{ratio} and penalty factor are refined for optimum solution by DCB model simulation and successfully used for simulation

of ENF and MMB test. Cohesive element response is defined by traction separation law. The material properties required to define traction separation law i.e. strength and stiffness are calculated using refined cohesive element parameters. A quadratic normal stress criterion is used for onset of delamination and subsequently B-K law is used for damage evaluation in numerical simulations. The cases analyse here are in good agreement with the test data and can be extended for progressive delamination/disbond determination in complex composite structures with mixed loading. The cases studied here are having pre-existing disbond; this approach can be extended to structure with without pre-existing disbond/delamination.

Acknowledgements

The authors thank Aeronautics Research & Development Board for sponsoring the work under ARDB Centre of Excellence in Composites Structures (ACECOST)-Phase III programme.

References

[1] A.J. Brunner, B.R.K. Blackman, P. Davies. A status report on delamination resistance testing of polymer matrix composites. Engineering Fracture Mechanics 75 (2008) 2779–2794
[2] Ronald Krueger. Virtual crack closure technique: History, approach, and applications. Appl Mech Rev vol. 57, no 2, March 2004.
[3] W. T. Chow, S. N. Atluri. Finite element calculation of stress intensity factors for interfacial crack using virtual crack closure integral. Computational Mechanics, November 1995, Volume 16, Issue 6, pp 417-425
[4] Zhou Hongliang. Calculation of stress intensity factors with the modified virtual crack closure technique. 18th International Conference on composite materials.
[5] N. Miyazaki, T. Watanabe, G. Yagawa. The virtual crack extension method for evaluation of J- and ĵ integral. Engineering Fracture Mechanics, Volume 22, Issue 6, 1985, Pages 975–987
[6] Goyal-Singhal, V., Johnson, E.R., Da´vila, C.G, and Jaunky, N. (2002). An Irreversible Constitutive Law for Modeling the delamination Process Using Interface Elements. 43rd AIAA/ASME/ASCE/AHS/ASC Structures, Structural Dynamics and Materials Conference, Colorado,USA.
[7] Albert Turon, Carlos G. Dávila, Pedro P. Camanho, Josep Costa. An Engineering Solution for using Coarse Meshes in the Simulation of Delamination with Cohesive Zone Models. NASA/TM-2005-213547.
[8] Diehl, T. Using ABAQUS Cohesive Elements to Model Peeling of an Epoxy-Bonded Aluminum Strip: A Benchmark Study for Inelastic Peel Arms. DuPont Engineering Technology, 2006, Abaqus Users Conference.
[9] ABAQUS Version 6.10 Documentation. Rhode Island, USA. : ABAQUS, Inc., 2010.
[10] ASTM D 5528, Standard test method for mode-I Interlaminar fracture toughness of unidirectional fibre reinforced polymer matrix composites, 2013.
[11] ASTM D 7905, Standard Test Method for Determination of the Mode II Interlaminar Fracture Toughness of Unidirectional Fiber-Reinforced Polymer Matrix Composites, 2014.
[12] ASTM D 6671, Standard Test Method for Mixed Mode I-Mode II Interlaminar Fracture Toughness of Unidirectional Fiber Reinforced Polymer Matrix Composites, 2013.
[13] S R Viswamurthy, S Nadeem Masood, M Siva, H V Ramachandra, “Interlaminar fracture toughness characterization of unidirectional carbon fiber composite (IMA/M21 prepreg)”, NAL Project Document PD-ACD/2013/1013, November 2013.
[14] M.L.Benzeggagh and M.Kenane, Mixed-mode delamination fracture toughness using MMB apparatus for unidirectional Glass/Epoxy. Composite Science and Technology, Vol.56, pp. 439-449, 1996.
[15] A Hillerborg, M Modeer and P-E Petersson. Analysis of crack formation and crack growth in concrete by means of fracture mechanics and finite elements. Cement and concrete research, Vol. 6, pp. 773-782, 1976.
[16] Song, S.H., Paulino, G.H., Buttlar, W.G. Simulation of crack propagation in asphalt concrete using an intrinsic cohesive zone model. Journal of Engineering Mechanics, vol. 132, no. 11, p. 1215-1223, DOI:10.1061/(ASCE)0733-9399(2006)132:11(1215)
[17] Zhang, Z.J., Paulino, G.H. Cohesive zone modelling of dynamic failure in homogeneous and functionally graded materials. International Journal of Plasticity, vol. 21, no. 6, p. 1195-1254, DOI:10.1016/j.ijplas. 2004.06.009.
[18] ABAQUS Version 6.5 Documentation. Rhode Island, USA. : ABAQUS, Inc., 2005.
[19] Diehl, T. Using ABAQUS Cohesive Elements to Model Peeling of an Epoxy-Bonded Aluminum Strip: A Benchmark Study for Inelastic Peel Arms. DuPont Engineering Technology, 2006, Abaqus users conference.
[20] Diehl, T. “On using a penalty-based cohesive-zone finite element approach, Part I: Elastic solution benchmarks” International Journal of Adhesion & Adhesives 28 (2008) 237–255.